

NASA TECHNICAL NOTE



NASA TN D-2739

NASA TN D-2739

LOAN COPY OF WORK  
FOR USE ONLY  
OF THE NATIONAL AERONAUTICS  
AND SPACE ADMINISTRATION

0079720



TECH LIBRARY KAFB, NM

# COMPARISON OF DIRECT AND INDIRECT ASCENT MODES FOR THE 1966-1967 MARS OPPORTUNITY WITH AN ATLAS-CENTAUR LAUNCH VEHICLE

*by Tim J. Kreiter*

*Lewis Research Center*

*Cleveland, Ohio*



0079710

NASA TN D-2739

COMPARISON OF DIRECT AND INDIRECT ASCENT MODES  
FOR THE 1966-1967 MARS OPPORTUNITY WITH AN  
ATLAS-CENTAUR LAUNCH VEHICLE

By Tim J. Kreiter

Lewis Research Center  
Cleveland, Ohio

NATIONAL AERONAUTICS AND SPACE ADMINISTRATION

---

For sale by the Office of Technical Services, Department of Commerce,  
Washington, D.C. 20230 -- Price \$1.00

# COMPARISON OF DIRECT AND INDIRECT ASCENT MODES FOR THE 1966-1967

## MARS OPPORTUNITY WITH AN ATLAS-CENTAUR LAUNCH VEHICLE

by Tim J. Kreiter

Lewis Research Center

### SUMMARY

A study has been made to determine the feasibility of using a direct ascent Atlas-Centaur booster to launch a flyby spacecraft to Mars during the 1966-1967 period. In order to evaluate the effectiveness of the direct ascent launching mode, daily launch windows and payloads were computed for both direct and indirect ascent trajectories and the two modes were compared on the basis of total number of launch opportunities and payload capability.

In this study, type I interplanetary transfer conics (heliocentric angles less than  $180^{\circ}$ ) were investigated over a three-month firing interval. A launch azimuth envelope of  $90^{\circ}$  to  $114^{\circ}$  was assumed, and a minimum daily launch window requirement of 60 minutes was imposed.

The direct ascent trajectories were selected such that the declination of the outgoing asymptote equaled the negative of the launch site (Cape Kennedy) latitude since this yielded near-maximum payloads. Indirect ascent trajectories were selected such that the daily launch energies were minimized. Launch windows were developed by varying injection flight path angle for direct ascent trajectories and by varying parking orbit coast time for indirect ascent trajectories.

The direct ascent mode was found not only to be feasible for a 1966 Mars flyby mission but also to be superior to the indirect ascent mode insofar as payloads and number of opportunities are concerned. For a 30-day launch period, a direct ascent Atlas-Centaur booster will deliver about 1480 pounds while an indirect ascent Atlas-Centaur booster will deliver about 1355 pounds.

### INTRODUCTION

Direct ascent Atlas-Centaur launch vehicles are presently being developed for the Surveyor program scheduled for the 1965-1966 time period. Since a Mars launch opportunity occurs in the 1966-1967 period, a study was made to determine whether direct

ascent Atlas-Centaur vehicles could also be utilized for this mission. Subsequent to this analysis, NASA decided not to launch a spacecraft to Mars with an Atlas-Centaur vehicle in 1966. The results of this study, however, are still significant inasmuch as a typical planetary flyby mission has been analyzed and a comparison has been made of the direct and indirect ascent launching modes.

Previous studies have recommended the use of the indirect or parking orbit ascent, and, in fact, the current Mariner C series, which is launched by Atlas-Agena vehicles, utilizes the indirect ascent mode. For indirect ascents, launch windows are developed by varying launch azimuth and parking time in orbit. The injection flight-path angle is at or near its optimum value, so that payload is nearly maximized.

For direct ascents, the degree of freedom provided by variable parking time is supplanted by the degree of freedom afforded by variable injection flight-path angles. The direct ascent mode is operationally simpler, inasmuch as there is no zero-gravity coast phase and no engine restart is required. The injection flight-path angles used in developing launch windows, however, must be near optimum to avoid serious degradation in payload.

In order to evaluate the effectiveness of the direct ascent mode, the direct ascent and parking orbit launch windows and payloads are compared for the 1966-1967 Mars opportunity.

Interplanetary trajectories may be classified into two general categories, namely, those for which the heliocentric travel angles are less than  $180^\circ$  (type I) and those for which the heliocentric travel angles are greater than  $180^\circ$  (type II) (ref. 1). In general, spacecraft designers prefer type I trajectories because they result in shorter trip times and lower communication distances at arrival. In the study reported herein, type I trajectories were investigated in the November, 1966 to February, 1967 interval, and trip times ranged from 207 to 246 days throughout the interval.

## SYMBOLS

$a, b, c, a', b', c'$	quadratic coefficients defined in appendix
$C_3$	geocentric vis viva injection energy
$d$	communication distance at arrival, AU
$g_c$	acceleration of gravity, $32.17 \text{ ft/sec}^2$
$I_{sp}$	specific impulse, seconds
$R_{inj}$	injection radius
$T_F$	time of flight, days

$T_L$	time of launch, hours past 0 <sup>h</sup> G. m. t.
$V_{cir}$	circular orbit velocity
$V_{inj}$	injection velocity
$W_{bo}$	burnout weight
$W_{ign, 1}$	ignition weight, 1st burn
$W_{ign, 2}$	ignition weight, 2nd burn
$W_{inj}$	injection weight
$\alpha$	booster powered flight arc
$\beta$	injection flight-path angle
$\epsilon$	total geocentric travel angle
$\Theta_L$	right ascension of the launch site at launch
$\Theta_S$	right ascension of the outgoing geocentric asymptote
$\kappa$	burnout ratio correction factor
$\lambda$	total polar angle
$\mu$	gravitational constant of the Earth, $3.986032 \times 10^5 \text{ km}^3/\text{sec}^2$
$\nu$	perigee-to-patch point angle
$\rho$	heading angle
$\Sigma$	launch azimuth angle
$\tau$	injection true anomaly
$T$	launch-site longitude ( $279.457^\circ$ East)
$\varphi_L$	launch-site latitude ( $28.317^\circ$ North)
$\varphi_S$	declination of the outgoing geocentric asymptote

## ANALYSIS

This study was divided into two phases; in the first phase, the appropriate Earth-to-Mars trajectories were determined, and in the second phase, the corresponding boost-vehicle payloads were calculated. The trajectory problem (of the first phase) was solved by assuming that the overall trajectory may be approximated by a geocentric conic and a heliocentric conic that are joined or patched at the Earth's sphere of influence.

Patched conic techniques for determining interplanetary trajectories are well known

and have been reported extensively (e.g., refs. 1 to 3). With the patched conic technique the equations relating trajectory parameters reduce to the well-known two-body equations and for brevity will not in general be repeated here.

The heliocentric conic trajectory was computed by first selecting a launch date and a trip time, which, in turn, define the positions of the Earth at launch and Mars at arrival. The unique conic trajectory was then found that passed through these two points and had the selected trip time. The actual calculations were performed by an iteration technique on a digital computer. Once the heliocentric conic was determined, the heliocentric departure conditions such as velocity, elevation angle, and so forth, were found by using the standard two-body conic equations.

These heliocentric departure conditions were used to derive important parameters for the geocentric conic trajectory. For example, the heliocentric departure velocity vector along with the Earth's orbital velocity vector were used to find the hyperbolic excess velocity vector and the direction (declination and right ascension) of the outgoing geocentric asymptote. The square of the hyperbolic excess velocity is known as the geocentric vis viva energy.

With vis viva energy and the outgoing asymptote defined, it was possible to design the geocentric conic trajectory. The first requirement of the geocentric conic trajectory was that it lie in a plane that passes through the launch site at launch and contains the outgoing asymptote.

In order to satisfy this planar orientation requirement, a spherical triangle was constructed on the celestial sphere such that the three apexes were (1) the north celestial pole, (2) the launch site zenith, and (3) the point in space defined by the asymptotic declination and the right ascension. The spherical triangle is shown in figure 1.

The spherical triangle is completely determined if three of the six spherical angles are known. Two angles are given or have previously been determined, namely, the launch site latitude  $\varphi_L$  ( $28.317^\circ$  North) and the declination of the outgoing asymptote  $\varphi_S$ , and a third angle remains to be chosen. In this study, the launch azimuth  $\Sigma$  was specified as the third spherical angle and was varied parametrically to develop the

launch window. The band of launch azimuths investigated was from  $90^\circ$  to  $114^\circ$ , which was assumed to typify Atlantic Missile Range (AMR) safety requirements.

The three remaining angles that were obtained by using the equations of spherical trigonometry are total geocentric travel angle  $\epsilon$  from launch to the Earth's sphere of influence (patch point), total polar angle  $\lambda$  from launch to patch point, and the heading angle  $\rho$

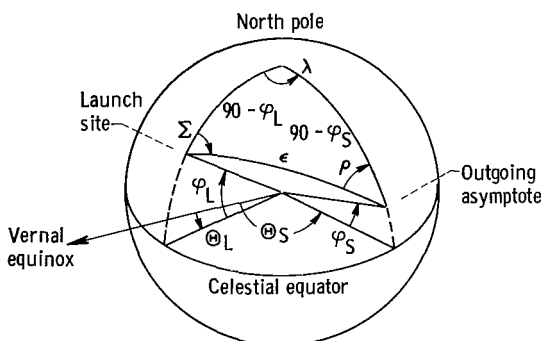


Figure 1. - Celestial sphere (Earth at center).

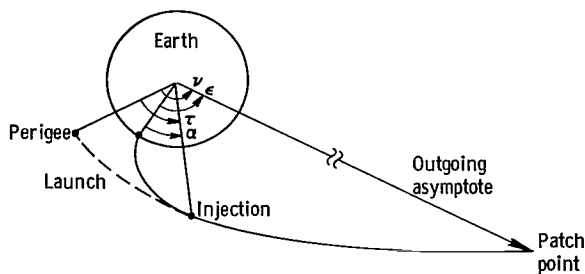


Figure 2. - Simplified planar geometry (direct ascent mode).

In figure 2, the relations among the total geocentric travel angle  $\epsilon$ , the booster-powered flight arc  $\alpha$ , the perigee-to-patch point angle  $\nu$ , and the injection true anomaly  $\tau$  are shown. For the indirect ascent mode, a geocentric parking arc (not shown in fig. 2) would also be present. The booster-powered flight arc was considered constant, and the perigee-to-patch point angle was found by using vis viva energy and the assumed perigee altitude of 90 nautical miles (ref. 1). Inasmuch as the booster-powered flight arc is assumed to lie in the plane of the geocentric conic trajectory, the injection true anomaly  $\tau$  may be found for the direct ascent mode as follows:

$$\tau = \alpha + \nu - \epsilon$$

The booster injection flight-path angle is found by using the injection true anomaly and the two-body conic equations.

The right ascension of the asymptote  $\Theta_S$  minus the total polar angle  $\lambda$  is equal to the right ascension of the launch site at launch  $\Theta_L$ . Launch time is computed by using the right ascension of the launch site at launch, launch site longitude ( $\Upsilon = 279.457^\circ$  East), the Greenwich hour angle at  $0^h$  Greenwich mean time of the launch date, and the rotation rate of the Earth (ref. 1).

In general, two solutions for launch time are obtained for a given launch azimuth (launch date and trip time), and this is attributable to the two possible solutions for the spherical triangle. The fact that two launch windows can exist on a given day is discussed in the section RESULTS AND DISCUSSION.

The digital computer program used to compute the heliocentric and geocentric conic trajectories in the first phase of this study was patterned very closely after that presented in reference 1. The main difference between the program used in this study and the one described in reference 1 is that the former used orbital elements (eccentricity, semimajor axis, orbital inclination to the ecliptic, longitude of the ascending node, argument of perihelion, and time of perihelion passage) to determine planetary positions whereas, in the latter, ephemerides were used.

In the second phase of this investigation, three of the geocentric conic trajectory parameters determined in the first phase namely, vis viva energy, injection flight-path

at the patch point (not used per se in this report). These angles were used, in turn, to determine the booster burnout or injection conditions (flight-path angle, altitude, etc.) and the time of launch. Once these quantities were determined, the design of the geocentric conic was considered complete.

In figure 2, the relations among the total geocentric travel angle  $\epsilon$ , the booster-

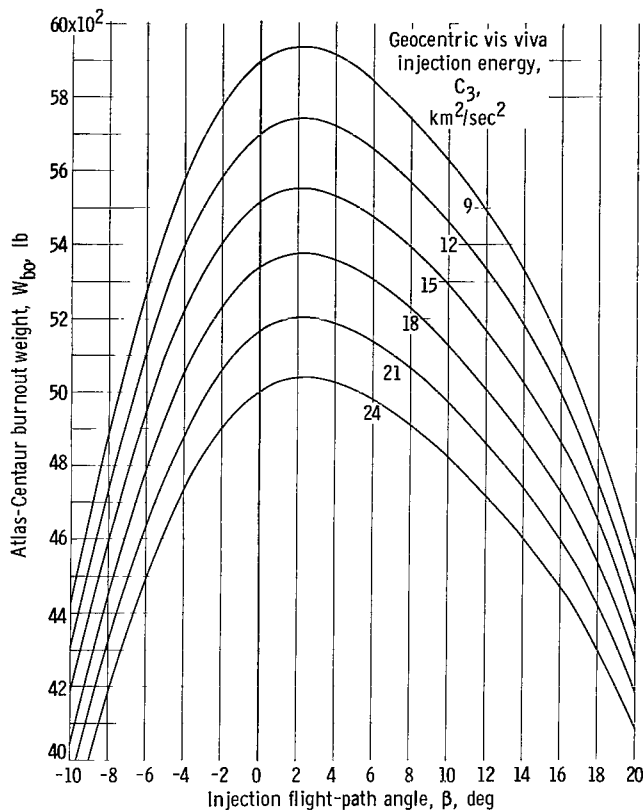


Figure 3. - Atlas-Centaur burnout weight as function of injection flight-path angle. Launch azimuth,  $102^\circ$ ; perigee altitude, 90 nautical miles.

angle, and launch azimuth, were used to derive Atlas-Centaur payload with the aid of booster performance curves. These curves present Atlas-Centaur burnout weights as functions of vis viva energy, injection flight-path angle, and launch azimuth. Payload is found by subtracting Centaur jettison weight from Atlas-Centaur burnout weight. The manner in which the booster performance curves were generated is discussed in the appendix.

In order to select trajectories that result in optimum vehicle performance for a given day, trip time was varied parametrically and the resulting payloads and launch windows were examined. Trip time is not selected in the same fashion for both the direct and indirect ascent modes because of the basic difference between the modes. These differences will be discussed in the following sections.

## Direct Ascent Mode

For the direct ascent launching mode, launch time, launch azimuth, and injection flight-path angle vary in a systematic manner throughout the launch window to satisfy the launch geometry requirements, which are continually changing because of the Earth's rotation.

Payloads for direct ascent trajectories were computed by using vis viva energy, injection flight-path angle, and launch azimuth; figure 3 shows Atlas-Centaur burnout weight plotted against injection flight-path angle for various vis viva energies and a launch azimuth of  $102^\circ$ . Observe how the burnout weight is penalized once the injection flight-path angle departs from its optimum value (about  $2^\circ$ ). Figure 4 shows the burnout ratio correction factor  $\kappa$  plotted against launch azimuth for a geocentric vis viva energy  $C_3$  of 12 kilometers squared per second squared and an injection true anomaly  $\tau$  of  $5^\circ$ . The burnout ratio correction factor was observed to be insensitive to geocen-



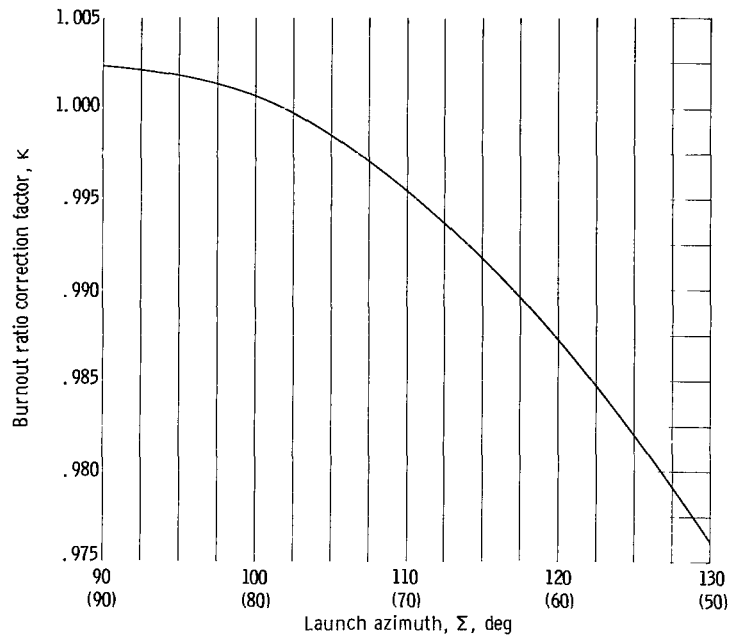


Figure 4. - Atlas-Centaur burnout ratio correction factor as function of launch azimuth. Geocentric vis viva injection energy, 12 kilometers squared per second squared; injection true anomaly,  $5^\circ$ .

tric vis viva injection energy  $C_3$  and injection true anomaly  $\tau$ . The burnout weights taken from figure 3 were multiplied by this ratio to make corrections for launch azimuths other than  $102^\circ$ .

In selecting a direct ascent trajectory for a given day, trip time was chosen so that the best compromise was achieved between payload and launch window. When this compromise is made, as will be demonstrated in the section RESULTS AND DISCUSSION, the resulting trajectories for all days in the launch interval exhibit the common property that the asymptotic declination is equal to the negative of the launch site latitude (i. e.,  $-28.317^\circ$ ).

The aforementioned results are based on the premises that launch azimuth is varied independently to develop daily launch windows and that, for a given day, trajectories will have constant trip times and vis viva energies. Another method of generating launch windows was discovered in the course of this analysis that involves launching at a constant azimuth; this scheme will be discussed briefly in the section RESULTS AND DISCUSSION.

## Indirect Ascent Mode

For the indirect or parking orbit ascent mode launch time, launch azimuth and parking time are varied systematically to meet launch geometry requirements. Note that

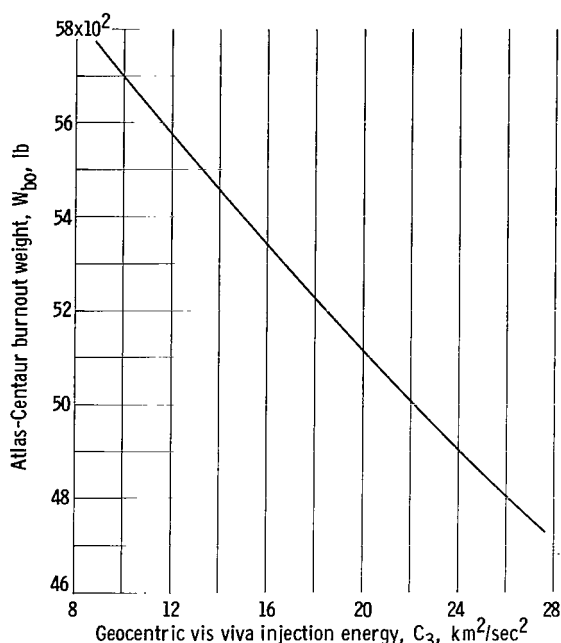


Figure 5. - Atlas-Centaur burnout weight as function of geocentric vis viva injection energy. Launch azimuth,  $114^\circ$ ; parking orbit coast time, 25 minutes; parking orbit altitude, 90 nautical miles.

parking time rather than injection flight-path angle provides the third degree of freedom. For indirect ascent trajectories, injection flight-path angle is selected to be near optimum in terms of payload.

Indirect ascent payloads are computed on the basis of vis viva energy, launch azimuth, and to a lesser extent by parking time inasmuch as parking time dictates the amount of cryogenic propellant boiloff occurring during the coast period. In this report a maximum parking time of 25 minutes and a launch azimuth of  $114^\circ$  were assumed in assessing indirect ascent payloads. This makes it possible to guarantee the widest daily launch windows over the entire launch interval since neither parking time was found to exceed 25 minutes throughout the interval nor was launch azimuth allowed to exceed  $114^\circ$ . Hence

for indirect ascent trajectories, payload was computed solely as a function of vis viva energy.

In figure 5 Atlas-Centaur burnout weight is shown as a function of vis viva energy for a parking time of 25 minutes and a launch azimuth of  $114^\circ$ . The details regarding the construction of figure 5 are given in the appendix.

For indirect ascent trajectories then, daily trip times were chosen such that vis viva energy was minimized, thereby optimizing payload.

## RESULTS AND DISCUSSION

### Direct Ascent Mode

For direct ascent trajectories the interrelation existing among trip time, launch azimuth, vis viva energy, asymptotic declination, flight-path angle, and payload are best demonstrated by examining a typical launch day in detail. Once these trends have been established, the entire launch interval may be discussed in terms of launch window and payload capability.

In figure 6, the injection flight-path angle and the launch azimuth are plotted against launch time for a typical day (Dec. 13) in the 1966-1967 Mars launch interval. The

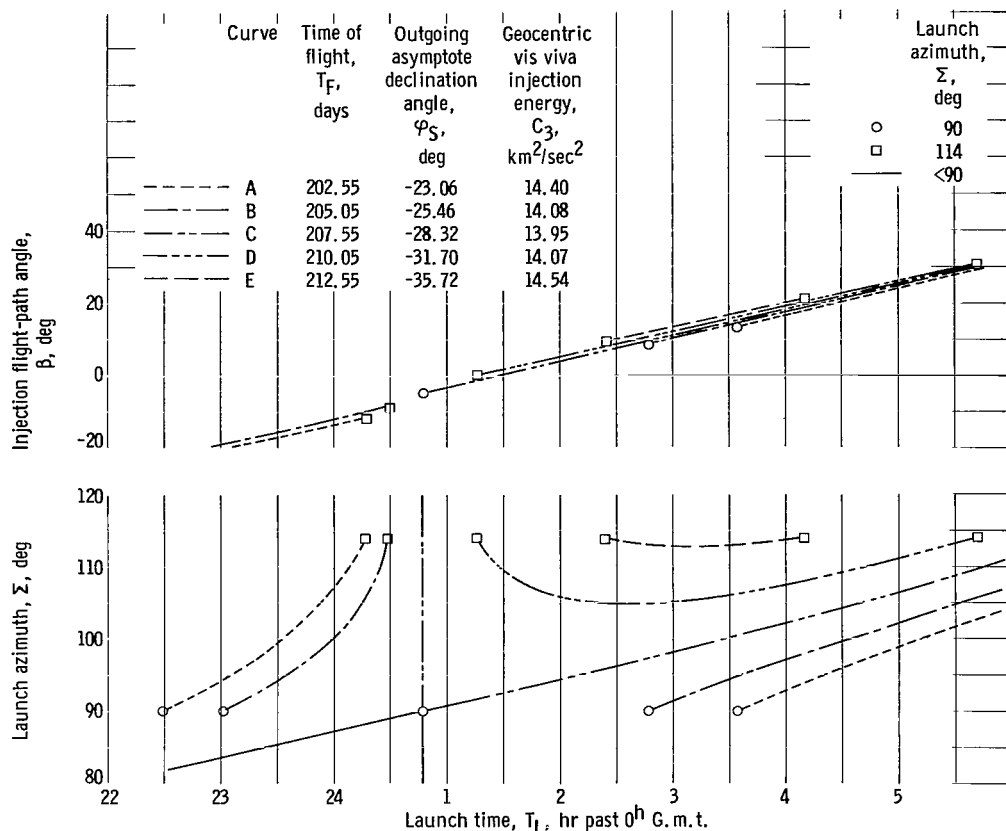


Figure 6. - Injection flight-path angle and launch azimuth as functions of launch time for type I direct ascent trajectories. Launch date: December 13, 1966.

curves in figure 6 represent trajectories with different trip times. For example, curve A represents a trajectory with a 202.55-day trip time, an asymptotic declination of  $-23.06^\circ$ , and a vis viva energy of 14.40 kilometers squared per second squared. Curve C depicts a trajectory for which the trip time has been chosen to make the declination of the outgoing asymptote equal to the negative of the launch site latitude. The circles represent launches made at  $90^\circ$  launch azimuth, while the squares represent launches made at  $114^\circ$ .

Curve C can be visualized to form a set of pseudoasymptotes. The solid portion of curve C represents launch azimuths less than  $90^\circ$ . Curve A and B are seen to have branches in the second and fourth quadrants as defined by the pseudoasymptotes. For all launch azimuths, there are two times during the day for which launches are feasible. Note that for curves A and B, the absolute value of the asymptotic declination is less than the launch site latitude.

On the other hand, curves D and E have branches in the first and third quadrants. The branches that occur in the third quadrant were not shown since the required launch

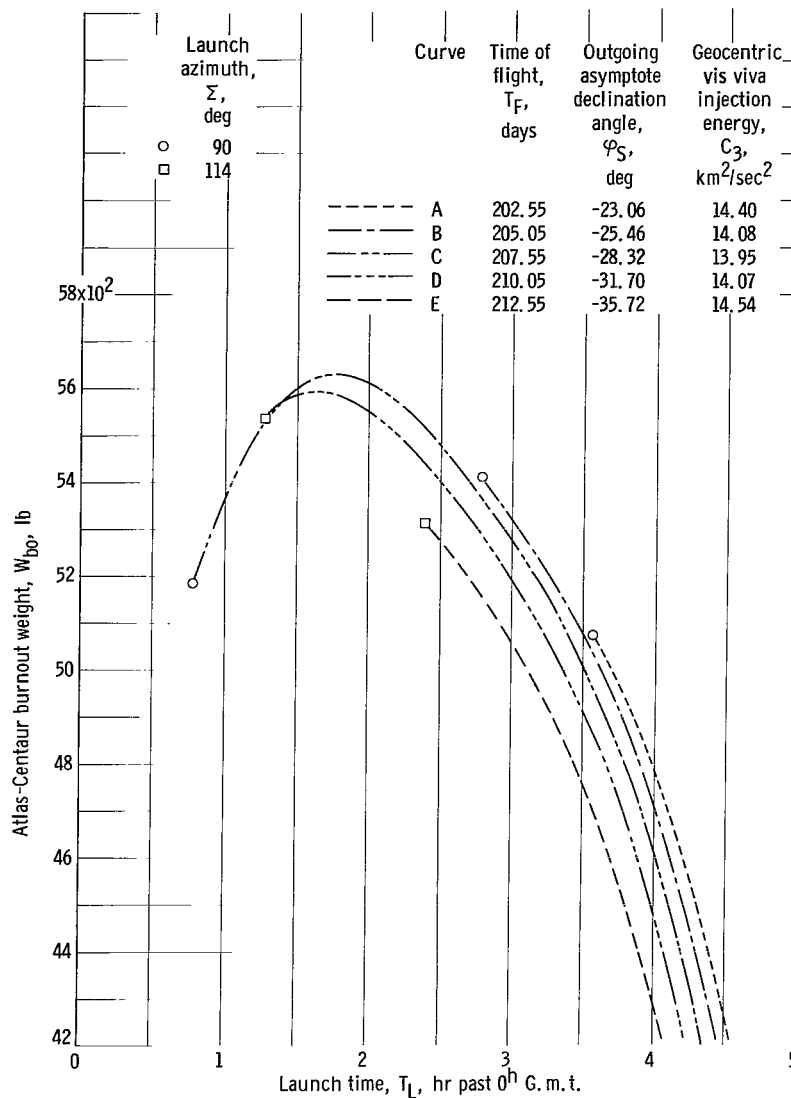


Figure 7. - Atlas-Centaur burnout weight as function of launch time for type I direct ascent trajectories. Launch date: December 13, 1966.

azimuths are considerably less than  $90^\circ$ . The maximum azimuths attained by the third quadrant branches for curves D and E are  $75.1^\circ$  at  $22^{\text{h}} 36^{\text{m}}$ , and  $67.3^\circ$  at  $21^{\text{h}} 35^{\text{m}}$ , respectively. Curves D and E represent trajectories for which the absolute value of the asymptotic declination exceeds the launch site latitude. In such a case (i. e., where  $|\varphi_S| > \varphi_L$ ), launches are not possible for certain launch azimuths. For curve D, the unusable azimuth zone extends from  $75.1^\circ$  to  $104.9^\circ$ ; for curve E, this zone lies between  $67.3^\circ$  and  $112.7^\circ$ . For the permissible launch azimuths, there are still two times during the day for which launches are feasible.

When the absolute value of the asymptotic declination exactly equals the launch site latitude ( $|\varphi_S| = \varphi_L$ ), a special case exists; curve C depicts this circumstance. At one

instant during the day, all launch azimuths satisfy the launch geometry requirements, as shown by the vertical portion of curve C. Otherwise, for a given launch azimuth, there is only one time during the day for which a launch is feasible.

In figure 6, the injection conditions are presented for the assumed launch date and trip time, but no information regarding payload capability is given. In figure 7, these injection conditions have been translated into payload capability via figures 3 and 4. Curves A to E represent burnout weights commensurate with trip times, injection flight-path angles, launch azimuths, and vis viva energies presented in figure 6.

The direct ascent launch windows and payloads used in this study are based on a choice of trip time that results in asymptotic declinations equal to the negative of the launch site latitude because this unique trip time results in a good compromise between payload and launch window as evidenced by curve C in figure 7. Justification for this method of selecting trip time lies in the fact that the same trends were observed for all other days investigated in the launch interval.

A surprising characteristic also shown in figure 7 is that more nearly optimum results could have been obtained if launches were always made at a launch azimuth of  $90^\circ$ . This characteristic was also found to be present for all other days examined in the launch interval. Although the fixed-azimuth launching technique was not investigated in detail, it could simplify tracking and range safety problems.

Data were obtained on the 1966-1967 Mars interval every 6 to 7 days beginning November 23, 1966 and ending February 15, 1967. Figure 8 shows the burnout weight variation with time for each of these days. The asymptotic declination was made equal

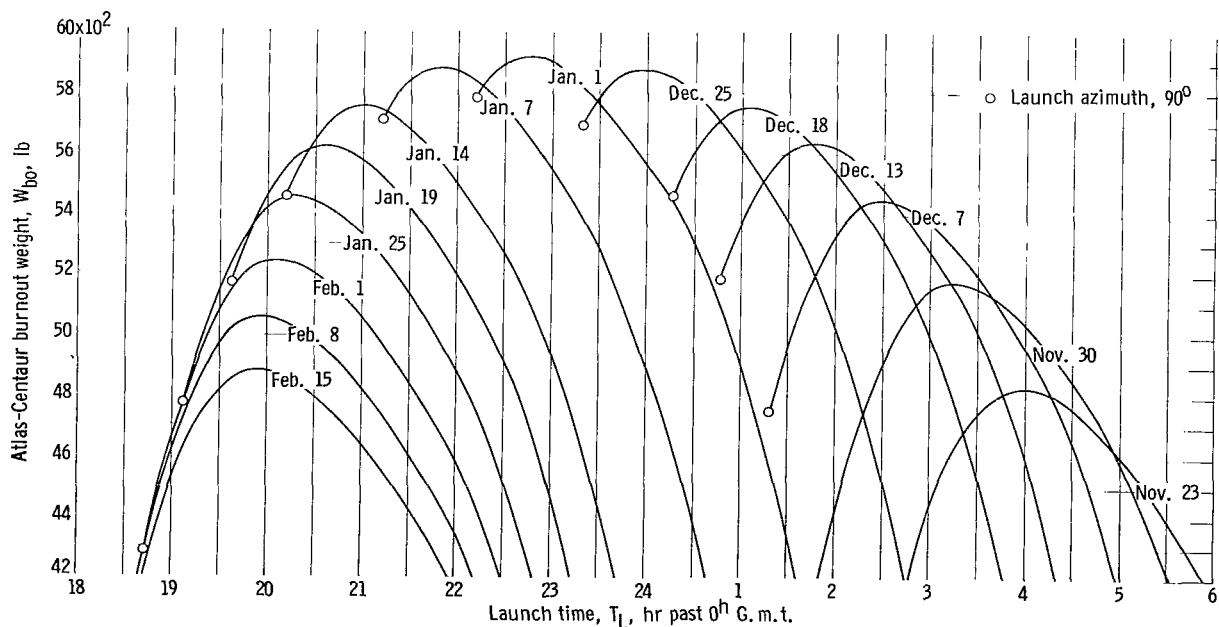


Figure 8. - Atlas-Centaur burnout weight as function of launch time for type I direct ascent trajectories. Launch interval: November 23, 1966 to February 15, 1967.

to the negative of the launch site latitude throughout the entire interval.

If payload (or burnout weight) were specified, a horizontal line could be drawn in figure 8 at that particular payload (or burnout weight) level. This line would, in general, intersect the daily burnout weight curves in two places corresponding to the time of window opening and the time of window closing. This time interval constitutes the launch window on the given day for a given payload. The time of window opening will in some cases be governed by the opening launch azimuth constraint ( $90^\circ$ ) indicated by the circles in figure 8. Figure 9, which was constructed in this fashion, presents daily launch windows plotted against date for curves of constant payload. Payload is equal to burnout weight minus Centaur jettison weight. The latter quantity was taken from reference 4. Observe that some of the launch window curves are depressed in the middle of the launch interval. This is a result of the  $90^\circ$  launch azimuth constraint.

## Indirect Ascent Mode

Figure 10 presents the payload and launch window capabilities afforded by the indirect or parking orbit ascent mode. In the indirect ascent analysis, daily vis viva energies were minimized and payloads were calculated by assuming both a 25-minute parking time and a  $114^\circ$  launch azimuth. (The longest parking times (up to 23 min) will occur in early February, while the shortest parking times (about 3 min) occur in mid-December.) The Centaur jettison weight was taken from reference 5. The indirect

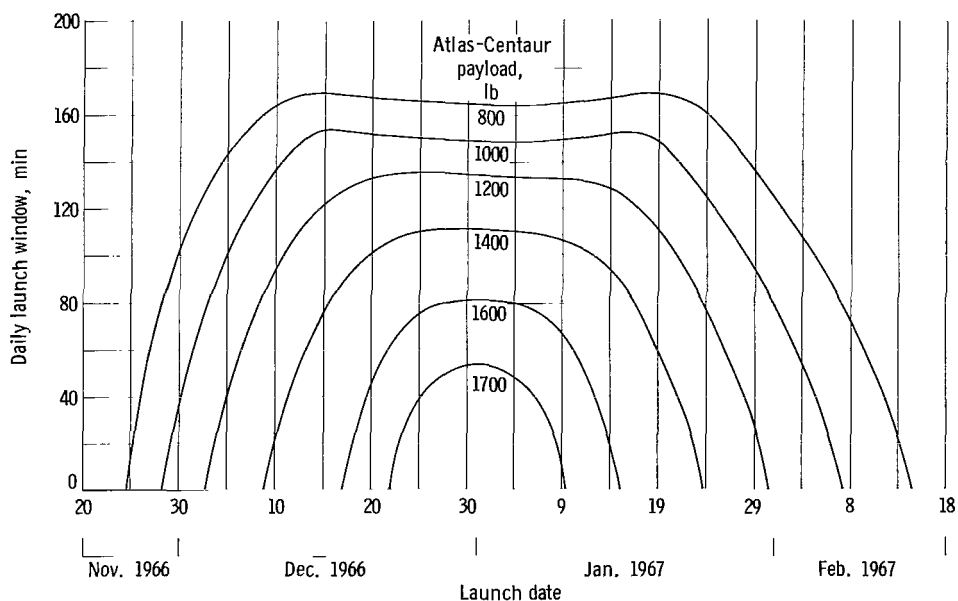


Figure 9. - Daily launch window as function of launch date for type I direct ascent trajectories. Launch interval: November 23, 1966 to February 15, 1967; Centaur jettison weight, 4142 pounds.

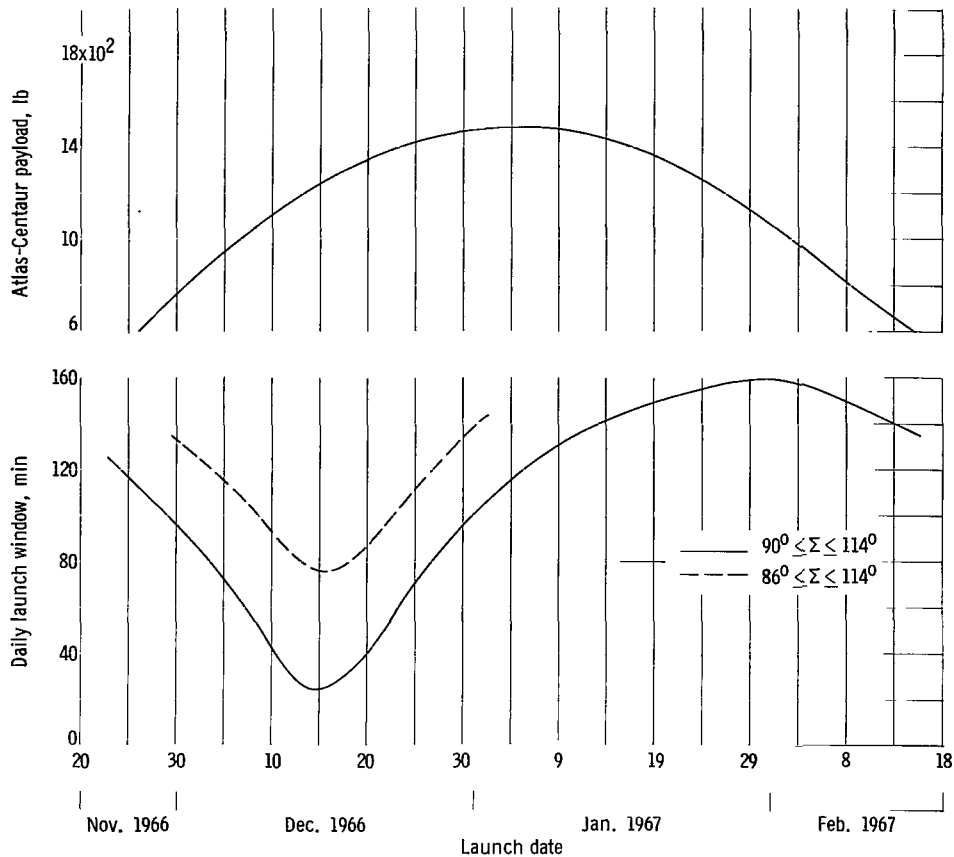


Figure 10. - Atlas-Centaur payload and daily launch window as functions of launch date for type I indirect ascent trajectories. Centaur jettison weight, 4275 pounds.

ascent technique is seen to provide fairly substantial launch windows over the entire launch period with the exception of a few days preceding or following December 15, 1966. On these occasions, the direct ascent mode provides the wider launch windows. This problem could be circumvented for the indirect ascent mode by relaxing the northerly launch azimuth constraint to  $86^\circ$ , for example, as shown by the dashed line in figure 10.

Vis viva energy, communication distance at arrival, and time of flight are shown as functions of launch date in figure 11. The solid lines represent direct ascent trajectories, that is, those for which the asymptotic declination equals the negative of the launch site latitude. The dashed lines represent indirect ascent trajectories or those for which the daily vis viva energy has been minimized. The trajectories for the direct and indirect ascent modes are similar until about December 30, 1966, after which the direct ascent mode is characterized by longer flight times, greater energies, and larger communication distances.

A comparison between the direct and the indirect ascent modes is presented in figure 12. Atlas-Centaur payload is shown as a function of the total number of launch opportunities. The solid line represents direct ascent trajectories with 60-minute mini-

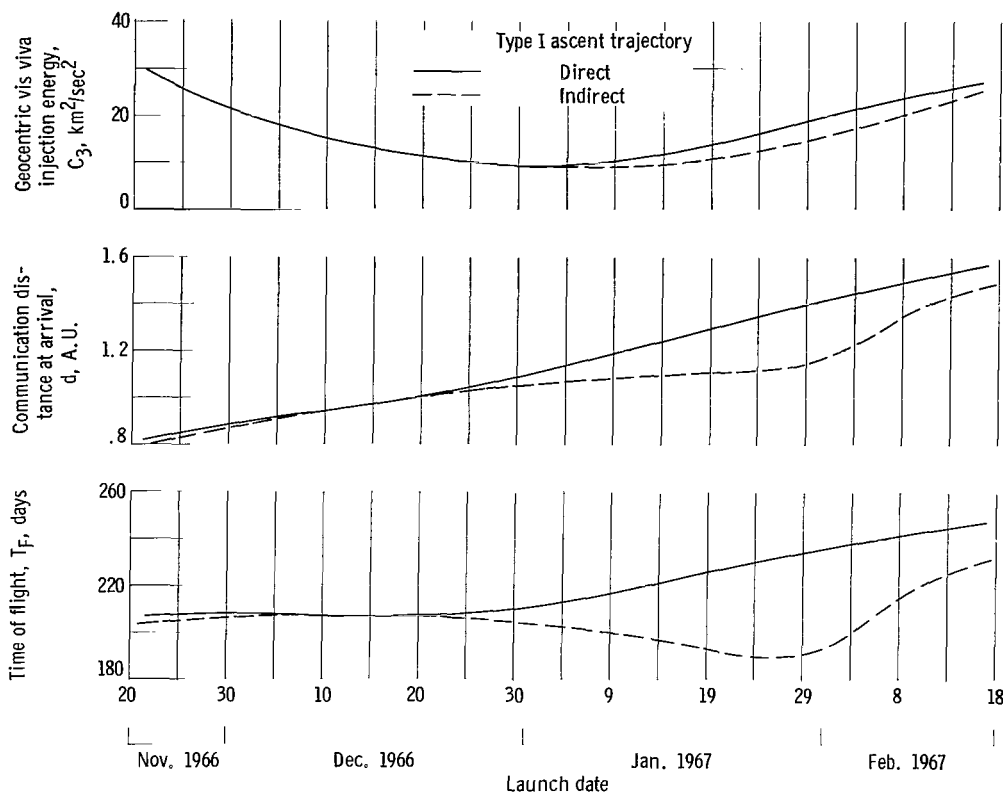


Figure 11. - Geocentric vis viva injection energy, communication distance at arrival, and time of flight as functions of launch date for type I direct and indirect ascent trajectories. Launch interval: November 23, 1966 to February 15, 1967.

mum daily launch windows. The dashed line represents indirect ascent trajectories with the northerly launch azimuth constraint having been relaxed in December to provide 60-minute windows. From figure 12 it can be seen that for a 30-day launch period the payload capability for direct ascent trajectories is 1480 pounds as compared to 1355 pounds for the indirect ascent trajectories indicating that the direct ascent mode is not only feasible for the 1966 Mars interval but is superior to the indirect ascent mode insofar as payloads and number of opportunities are concerned.

## CONCLUDING REMARKS

From this study in which the effectiveness of the direct ascent launching mode for planetary flyby missions was evaluated, it may be concluded that:

1. Type I trajectories for the Mars 1966-1967 launch interval lend themselves to the direct ascent launching mode for the Atlas-Centaur vehicle.
2. Direct ascent payloads and daily launch windows are nearly optimized when trip times are chosen that make the asymptotic declinations equal to the negative of the



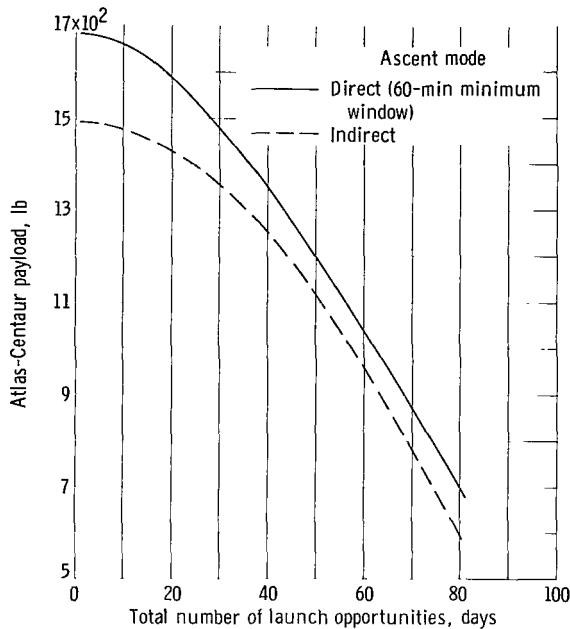


Figure 12. - Atlas-Centaur payload as function of total number of launch opportunities for Mars 1966 - 1967 launch interval, type I trajectories.

launch site latitude.

3. For a minimum daily launch window of 60 minutes and a launch period of 30 days (Dec. 16 to Jan. 15), the Atlas-Centaur will deliver a gross payload of about 1480 pounds via the direct launching mode. As a point of comparison, the indirect launching mode (parking orbit) provides about 1355 pounds for a 30-day period (Dec. 20 to Jan. 19).

An interesting sidelight of this study for the direct ascent mode is the possibility of launching at a fixed azimuth ( $90^{\circ}$ ). Only a cursory examination of this phenomenon was made in this analysis, but inasmuch as the payloads and launch windows resulting from fixed azimuth launches were more nearly optimum for the Mars 1966 opportunity, a more detailed look at this concept might be rewarding.

Although the direct ascent mode appeared favorable for the 1966 Mars mission investigated in this report, it should not be concluded that the direct ascent mode would always be favorable. As a matter of fact, a preliminary study of the 1969 Mars opportunity revealed that the indirect ascent mode was more attractive for this opportunity. Each planetary launch opportunity must be examined individually in order to arrive at the best choice of ascent mode.

In the foregoing analysis, trajectories were selected to maximize launch vehicle performance. The spacecraft was assumed to be of the flyby type, and no special spacecraft constraints were considered.

Lewis Research Center,  
National Aeronautics and Space Administration,  
Cleveland, Ohio, December 7, 1964.

## APPENDIX - BOOSTER PERFORMANCE ASSUMPTIONS

The performance curves for the Atlas-Centaur booster shown in figures 3 to 5 (pp. 6 to 8) were obtained by using a simplified booster program developed at the Lewis Research Center. The booster flight profile was characterized by a short vertical rise followed by a zero angle of attack trajectory throughout the booster portion of the Atlas burning phase. An optimized steering program using calculus of variations was followed during the Atlas sustainer and Centaur burning phases. This program is not as detailed as the precision booster programs used for the analysis of Surveyor launch trajectories; however, it is faster and more convenient to use. The simplified program is sufficiently accurate for preliminary performance (payload) calculations particularly for missions wherein the vehicle and mission input data, in themselves, are not precisely defined.

The direct ascent data and the indirect ascent data were not generated at the same time, and consequently, two references are quoted herein for booster vehicle data and Centaur jettison weights. Reference 4 was used when the direct ascent data were derived, and reference 5 was used to derive the indirect ascent data. Inasmuch as the minimum burnout and Centaur jettison weights for a direct ascent vehicle (Atlas-Centaur 7) only changed -3 and 6 pounds respectively, between references 4 and 5, it is felt that a fair comparison has been made.

### Direct Ascent Payload Computation

Figure 3, which was obtained by using the simplified program, shows Atlas-Centaur burnout weight plotted against the injection flight-path (elevation) angle for constant vis viva energies. The data were generated for perigee altitudes of 90 nautical miles and a launch azimuth of  $102^\circ$ . Booster vehicle data used in the simplified booster program were taken from reference 4. Figure 4 shows the burnout ratio correction factor  $\kappa$  plotted against azimuth. For azimuth headings other than  $102^\circ$ , the burnout weight is multiplied by this ratio.

The digital computer program used to generate the Earth-to-Mars trajectories possessed the capability of simultaneously calculating booster burnout weight for each trajectory. This was accomplished by approximating the burnout weight against injection flight-path angle curve with a number of curve segments of the form

$$W_{bo, 102^\circ} = a + b\beta + c\beta^2 \quad (A1)$$

where  $W_{bo, 102^\circ}$  is the Atlas-Centaur burnout weight for a launch azimuth of  $102^\circ$

(and a given vis viva energy),  $\beta$  is the injection flight-path angle, and  $a$ ,  $b$ , and  $c$  are the quadratic coefficients in the flight-path angle region of interest. The burnout weight was computed at integral vis viva energies above and below the desired value, and a linear interpolation was made.

Likewise, the burnout ratio correction factor curve was approximated by a series of curve segments of the form

$$\kappa = \frac{W_{bo}}{W_{bo, 102^\circ}} = a' + b'\Sigma + c'\Sigma^2 \quad (A2)$$

where  $W_{bo}$  is the burnout weight for the given launch azimuth  $\Sigma$  and  $a'$ ,  $b'$ , and  $c'$  are the quadratic coefficients for the particular azimuth regime being considered.

Payload was found by subtracting the Centaur jettison weight from the burnout weights as derived in the manner described previously. In this analysis, a Centaur jettison weight of 4142 pounds (Atlas-Centaur 7) was assumed, which includes 180 pounds of flight performance reserves (ref. 4).

## Indirect Ascent Payload Computation

The indirect ascent payloads were calculated in two steps. In the first step, the

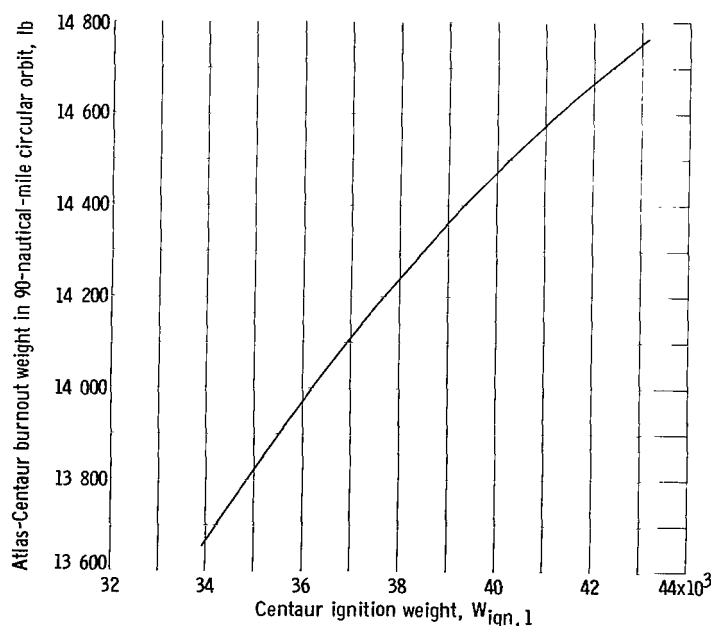


Figure 13. - Atlas-Centaur burnout weight in 90-nautical-mile orbit as function of Centaur ignition weight. Launch azimuth,  $102^\circ$ .

simplified booster program flew the Atlas-Centaur to a 90-nautical-mile circular orbit for a specific Centaur ignition weight, computing burnout weight in circular orbit and the amount of Centaur propellant consumed during first burn. Inasmuch as full propellant tanks were assumed, the propellant available for second burn may be computed by subtracting the amount of first burn propellant plus any weight penalties (boiloff, chilldown, leakage, etc.) incurred during coast from the amount of total usable propellant. The second burn ignition weight is equal to the burnout weight in circu-

lar orbit minus the coasting penalties.

In the second step, the second burn ignition weight and the weight of remaining propellants were used in the well-known characteristic velocity equation to derive the final burnout weight. The process was repeated for various Centaur ignition weights.

Figure 13 shows the Atlas-Centaur burnout weight in a 90-nautical-mile circular orbit as a function of Centaur ignition weight for a launch azimuth of  $102^\circ$ .

The total usable propellant was assumed to be 29 882 pounds and was computed as follows:

Main impulse propellants, lb . . . . .	30 021
Flight performance reserves, lb . . . . .	-180
Hydrogen peroxide consumed during the first and second burning periods (35 and 21 lb, resp.), lb . . . . .	56
Hydrogen vented for extra 5 minutes of coast (ref. 5 depicted 20-min coast period), lb . . . . .	-15
Total usable propellant, lb . . . . .	29 882

The amount of propellant used during first burn was assumed to be equal to the Centaur ignition weight minus 0.99286 (azimuth correction factor for  $114^\circ$  launch azimuth) times the circular orbit weight given in figure 13 plus the weight of hydrogen peroxide ( $H_2O_2$ ) consumed during first burn (35 lb).

The following quantities (taken from ref. 5) were then subtracted to derive the second burn ignition weight  $W_{ign, 2}$

Engine shutdown loss, lb . . . . .	16
Propellant leakage, lb . . . . .	2
Hydrogen vented during coast (linearly increased to account for 25-min coast), lb . . . . .	77
Engine chutdown propellant loss, lb . . . . .	31
Hydrogen peroxide consumed for ullage during coast (linearly increased to account for 25-min coast), lb . . . . .	45
Total weight penalty incurred, lb . . . . .	171

Since the total amount of usable propellants and the amount of propellant consumed during first burn are known, the propellants available for the second burn may be found by subtracting the two. The injection weight  $W_{inj}$  is then equal to the second burn ignition weight minus the propellants consumed during second burn minus the  $H_2O_2$  used during velocity trim (6 lb).

To find injection velocity, the following characteristic velocity equation is used:

$$V_{inj} = V_{cir} + g_c I_{sp} \ln \frac{W_{ign, 2}}{W_{inj}} \quad (A3)$$

where the specific impulse (degraded to include the effect of  $H_2O_2$  by assuming  $I_{sp} = 430(30\ 021 - 180) (30\ 021 - 180 + 56)$ ) is  $I_{sp} = 429.19$  seconds.

The vis viva energy is equal to  $V_{inj}^2 - 2\mu/R_{inj}$  where  $\mu$  is the gravitational constant of the Earth and  $R_{inj}$  is the injection radius. Figure 5 was developed by making use of figure 13 and the aforementioned procedures.

From reference 5 the Centaur jettison weight for parking orbit Centaur (viz, Atlas-Centaur 12) is 4555 pounds, which includes 180 pounds of flight performance reserves. The Atlas-Centaur 12 is a research and development vehicle, and the useful instrument load (774 lb) is considerably more than that of an operational vehicle such as the Atlas-Centaur 7 (494 lb). The jettison weight assumed herein (4275 lb) was derived by adjusting the Atlas-Centaur 12 jettison weight to reflect an operational rather than a research and development instrument load. The following steps summarize these calculations:

Atlas-Centaur 12 jettison weight (including

flight performance reserves), lb . . . . .	4555
Instrument load adjustment, lb . . . . .	-280
Parking orbit jettison weight, lb . . . . .	4275

where the instrument load adjustment was calculated as follows:

Atlas-Centaur 12 useful load (research

and development vehicle), lb . . . . .	774
Atlas-Centaur 7 useful load (operational vehicle), lb . . . . .	-494
Instrument load adjustment, lb . . . . .	280

## REFERENCES

1. Clarke, V. C., Jr.; Bollman, W. E.; Roth, R. Y.; and Scholey, W. J.: Design Parameters for Ballistic Interplanetary Trajectories. Pt. 1. One-Way Transfers to Mars and Venus. TR 32-77, Jet Prop. Lab., C.I.T., Jan. 16, 1963.
2. Knip, Gerald, Jr.; and Zola, Charles L.: Three-Dimensional Sphere-of-Influence Analysis of Interplanetary Trajectories to Mars. NASA TN D-1199, 1962.
3. Lorell, J.; and Oster, C.: A Patched Conic Computation Program for Interplanetary Trajectories. Memo. 30-10, Jet Prop. Lab., C.I.T., Sept. 30, 1959.
4. Zobal, S. A.: Centaur Monthly Configuration, Performance and Weight Status Report. GDA 63-0495-8, Convair Astronautics, Jan. 21, 1964.
5. Zobal, S. A.: Centaur Monthly Configuration, Performance and Weight Status Report. GDA 63-0495-9, Convair Astronautics, Feb. 21, 1964.



2/22/85  
of

*"The aeronautical and space activities of the United States shall be conducted so as to contribute . . . to the expansion of human knowledge of phenomena in the atmosphere and space. The Administration shall provide for the widest practicable and appropriate dissemination of information concerning its activities and the results thereof."*

—NATIONAL AERONAUTICS AND SPACE ACT OF 1958

## NASA SCIENTIFIC AND TECHNICAL PUBLICATIONS

**TECHNICAL REPORTS:** Scientific and technical information considered important, complete, and a lasting contribution to existing knowledge.

**TECHNICAL NOTES:** Information less broad in scope but nevertheless of importance as a contribution to existing knowledge.

**TECHNICAL MEMORANDUMS:** Information receiving limited distribution because of preliminary data, security classification, or other reasons.

**CONTRACTOR REPORTS:** Technical information generated in connection with a NASA contract or grant and released under NASA auspices.

**TECHNICAL TRANSLATIONS:** Information published in a foreign language considered to merit NASA distribution in English.

**TECHNICAL REPRINTS:** Information derived from NASA activities and initially published in the form of journal articles.

**SPECIAL PUBLICATIONS:** Information derived from or of value to NASA activities but not necessarily reporting the results of individual NASA-programmed scientific efforts. Publications include conference proceedings, monographs, data compilations, handbooks, sourcebooks, and special bibliographies.

*Details on the availability of these publications may be obtained from:*

SCIENTIFIC AND TECHNICAL INFORMATION DIVISION  
NATIONAL AERONAUTICS AND SPACE ADMINISTRATION  
Washington, D.C. 20546